RESEARCH ARTICLE

A Novel Suberoylanilide Hydroxamic Acid Histone Deacetylase Inhibitor Derivative, N25, Exhibiting Improved Antitumor Activity in both Human U251 and H460 Cells

Song Zhang[1], Wei-Bin Huang[1], Li Wu[1, 2], Lai-You Wang[1], Lian-Bao Ye[1], Bing-Hong Feng[1]*

Abstract

N^1- (2, 5-dimethoxyphenyl)-N^8-hydroxyoctanediamide (N25) is a novel SAHA cap derivative of HDACi, with a patent (No. CN 103159646). This invention is a hydroxamic acid compound with a structural formula of RNHCO(CH_2)6CONHOH (wherein R=2, 5dimethoxyaniline), a pharmaceutically acceptable salt which is soluble. In the present study, we investigated the effects of N25 with regard to drug distribution and molecular docking, and anti-proliferation, apoptosis, cell cycling, and LD_{50}. First, we designed a molecular approach for modeling selected SAHA derivatives based on available structural information regarding human HDAC8 in complex with SAHA (PDB code 1T69). N25 was found to be stabilized by direct interaction with the HDAC8. Anti-proliferative activity was observed in human glioma U251, U87, T98G cells and human lung cancer H460, A549, H1299 cells at moderate concentrations (0.5-30μM). Compared with SAHA, N25 displayed an increased antitumor activity in U251 and H460 cells. We further analyzed cell death mechanisms activated by N25 in U251 and H460 cells. N25 significantly increased acetylation of Histone 3 and inhibited HDAC4. On RT-PCR analysis, N25 increased the mRNA levels of p21, however, decreased the levels of p53. These resulted in promotion of apoptosis, inducing G0/G1 arrest in U251 cells and G2/M arrest in H460 cells in a time-dependent and dose-dependent manner. In addition, N25 was able to distribute to brain tissue through the blood-brain barrier of mice (LD_{50}: 240.840mg/kg). In conclusion, our findings demonstrate that N25 will provide an invaluable tool to investigate the molecular mechanism with potential chemotherapeutic value in several malignancies, especially human glioma.

Keywords: N25 - histone deacetylase inhibitor (HDACi) - anti-tumor activity - human U251 - H460 cells

Asian Pac J Cancer Prev, **15 (10)**, 4331-4338

Introduction

A mass of research have demonstrated that epigenetic gene modulation has been postulated to be an essential mechanism in cancer development and metastasis (Nelson et al., 2012). The modification of histone acetylation plays a critical role in epigenetics as the hotspot of international research (Sriraksa et al., 2013). Especially in histone tails the reversible acetylation of lysine residues has been a key part of activation and repression in transcriptional. The state of histone acetylation is balanced by the opposing activities of histone acetyltransferase (HATs) and histone deacetylase (HDACs) that induces the regulation of post-translational modifications (Hoshino et al., 2010; Duo et al., 2013). Enhanced HDAC activity represses transcriptional of many genes related to differentiation and tumor suppressor genes in cancer cells. Thus, the increased activity of HAT (or HDAC inhibition) promotes gene expression (Hoshino et al., 2007; Ellis et al., 2008), which was a primary process of normal cell growth and differentiation. Although the mechanisms of HDACis effect these antitumor activities have not been fully demonstrated, induction of histone hyper acetylation and modulation of gene transcription through chromatin remodeling are generally to be chiefly responsible (Dubois et al., 2009).

In this context, suberoylanilide hydroxamic acid (Vorinostat, SAHA) is the first HDACi appeared as an anticancer effective and gained FDA approval for the treatment of advanced cutaneous T-cell lymphoma in 2006 (Al-Yacoub et al., 2012). Most compounds of HDACi are closely similar the aliphatic acetyl-lysine structure. Synthetic analogs isolated from screening libraries are discovered to have a common structure with TSA and SAHA i.e. A hydroxamic acid bingding group linked via a spacer (5 or 6 CH_2) to a hydrophobic group. Co-crystallization of these agents deliver an hydroxamic acid moiety or other zinc- binding group to the catalytic

*[1]Department of Pharmacology, College of Pharmacy, Guangdong Pharmaceutical University, [2]Guangdong Food and Drug Vocational-technical School, Guangzhou, China *For correspondence: fengbh@gdpu.edu.cn, fengbh2010@163.com*

zinc ion at the bottom of a narrow active site pocket resulting in the inhibition of HDAC activity, observed in co-crystal structures of human HDAC8 (Di Fiore et al., 2012). Furthermore changing the metal-binding moiety part for a HDACi design, the hydrocarbon linker has been diversified to focus on altering chain length, the creation of unsaturation points along the chain, and the inclusion of a ring structure within the chain. For this reason, dividing into three charactreristic groups of SAHA as a HDAC inhibitors model have included a metal binding moiety, carbon linker, and capping group.

In the integrated analysis of crystallographic, close the inlet of the active site have amino acids induced capping part is coalesce-exposed and interacts. Conversely, the metal-binding moiety inserted in the protein interior and chelate with the zinc ion at the bottom of a narrow active site pocket. But, the effect of substituent of the SAHA phenyl capping group still unclear, most probable because the synthesis schemed have precluded such analogues from being easily produced. Multiple regulation of HDACs resulted in the side effect of SAHA. These might be the reason of the effect of substituent of the SAHA phenyl capping group. However, a small amount of program for the design of capping group derivatives has been expected and less evaluation of their potent biological activities has been described. Although several unpublished variations of the SAHA structure seem to have been developed, these were too toxic to be considered as potential drug candidates (Finnin et al., 1999; Takai et al., 2011; Di Micco et al., 2013). We need more novel HDACis.

In this study, we present a novel compound N25 produced by a moderate two-step synthesis with commercially cheap available reagents (Scheme 1). Replaced a hydrophobic capping group with high-yield synthesis. While this modification might not be considered particularly new, as we know, the influence of the capping group substitution in the antitumoral selectivity remains unclear and a few studies have examined the impact of N25 on its biological activities. Against all expectations, observed selective promotion in the anti-gilomas activity of some of these SAHA analogues.

Materials and Methods

Chemistry synthesis and structural identification

The general synthetic strategies shown in Schemes 1 were employed for the preparation of the new hydroxamic acids N25. The first step consists of a typical peptide coupling reaction using a commercial available suberic acid monomethyl ester and 2, 5-dimethoxy-anilin for amide bond formation with an efficient and (Benzotriazol1yloxy) tris (dimethylamino) phosphonium hexafluophosphate couplingreagent (BOP) and diisopropylethyl-amine (DIEA) in CH_2Cl_2. The mixture was stirred at room temperature for 24h. The product was obtained by spin steaming wipe out CH_2Cl_2, and crude product was dissolved in petroleum ether and ethyl acetate (20:1) and then filtered through a short pad of silica gel. Thus, the product (2) was obtained in 32.88% yield. The obtained ester was successful transformed into its corresponding hydroxamic derivative by using hydroxylamine, which was prepared by mixing hydroxylamine hydrochloride with sodium hydroxide in methanol. The freshly prepared hydroxylamine was stirred at room temperature with (2) for 2h. The product was obtained by adding water and neutralizing with acetic acid to obtain N25 in 20.0% yield (96.266%) purity as determined by HPLC. The structure was identified by ^{1}HNMR and MS (ESI$^+$). N25 was fully characterized by physical and spectral methods and compared with literature data of SAHA.

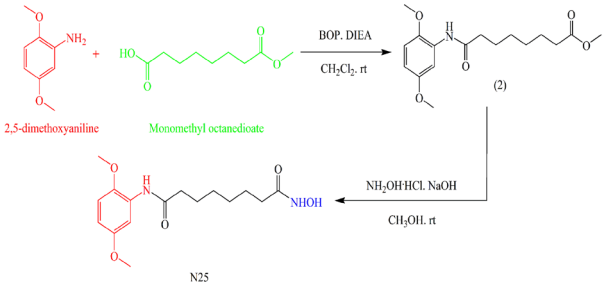

Scheme 1. General Pathway for N25 Synthesis

Reagents

N25 was supplied by our subject dissolved in anhydrous dimethyl sulfoxide (DMSO). For the experiments, N25 was configuration in 5, 10, 20, 40, 80, 160, 320μM with Serum-free DMEM medium or RPMI 1640 medium. SAHA purchased from Guangzhou QiYun biological technology co., LTD.

Docking analyze

AutoDock 4 actually consists of two main programs: autodock performs the docking of the ligand to a set of grids describing the target protein; autogrid pre-calculates these grids. We employed these tools to study the free energy and residues participating in hydrophobic interactions. Pymol software analyzed hydrogen bond and mark hydrophobic interact amino acids. Chimera software showed hydrophobic interactions (Li et al., 2013).

Cell lines and cell culture

The human glioma cell line U251, U87, T98G cells and human lung cancer H460, A549, H1299 cells were kindly provided by Sun Yat-Sen University Cancer Center. The cells were from -80°C cryogenic refrigerator quickly thawed in constant temperature water bath (37°C) divided supernate and cultured in RPMI 1640 containing 10% FBS (fetal bovine serum). The cells were respectively in 25cm^2 cell culture bottle for 5% CO_2 at 37°C, harvested with 1 ml 0.25% trypsin and then resuspended in fresh medium.

Determination of cell proliferation

Cells (1x10^4) were incubated 90μl of culture medium for 24h in 96-well plates, and treated with various concentration (0.5, 1, 2, 4, 8, 16, 32μM) of N25 solution 10μl for the each well. After 48h of incubation, 10μl of Cell Counting Kit (CCK8) was added and cells then incubated at 37°C for 1h. The plate was read with a microplate reader (Bio-Rad Laboratories, Hercules, CA, USA) at 490nm. The inhibition rate of cell proliferation was determined by the equation (1-ODtreated/ODcontrol)×100. OD is

the average of three optical number from the reader. N25 first examined for cell proliferation, inhibited U251, U87, T98G and H460, A549, H1299 cell line proliferation, with IC_{50} values varying from 4% to 75%. In contrast, SAHA displayed the weakest anti-proliferative activity, with U251, H460, A549, H1299 cell line; better in U87, T98G. As expected, the anti-proliferative activity of the N25 compound correlated well with the cap modified.

Cell-cycle analysis

The cells were treated with N25 for the indicated times, fixed with 75% (v/v) ethanol and stained with 50μg/ml PI (propidium iodide) containing 100μg/ml RNaseA, for 1h. The percentages of cells in different cell cycle phases were measured using a fluorescen-activated cell flow cytometer (Beckman FC500/COULTER EPICS X FCM, Beckman Coulter, Inc. USA). Built the PT-PCR reaction system and program and used agarose gel electrophoresis to detect RT-PCR products.

Immunoblotting Assay of HDAC activity

HDAC activity was detected by Followed the specification of BCA protein concentration determination kit, purchased from BiYunTian biotechnology research institute. Each reaction (100μl) contained protein (50μg) extract from H460 and U251 cells. To exam the influnce of HDACis, N25 and SAHA were respectively added to the mixtures and cultivated at 37°C for 48h. Treated and untreated cells were harvested with trypsin-EDTA, washed with PBS, and resuspended in a protein sample buffer. The results of HDAC activities were tested by an ELIASA (Bio-Rad corporation) at 570nm. HDAC expression profile between H460 and U251 tumor-derived cell lines. N25 was compared to SAHA in a deacetylase activity assay using cell-derived HDAC4, H3 (K9+K14+K18+K23+K27) and H3-K9.

Western blotting

After 48h different treatments, as described in the instructions, the cells were washed twice in PBS, suspended in lysis buffer (every 250μl containing 1mM PMSF, Bi Yun Tian biotechnology research institute) on ice for 5min. After centrifuged at 14000g for 5min at 4°C, the suspension was collected. In each sample, the protein concentration were quantified by a BCA assay (Bi Yun Tian biotechnology research institute). In U251 total loaded 80μg and in H460 total loaded 150μg, equivalent protein were resolved by SDS/PAGE, electrotransferred to a PVDF membrane and probed sequentially with antibodies. Detection was performed using chemiluminescent ECL (Pierce) substrate. The antibodies used as following: anti-[acetyl-histone H3-K9], anti-[acetyl-histone H3- K9+K14+K18+K23+K27] and total anti- (histone H4), anti-GAPDH (glyceraldehyde-3-phosphate dehydrogenase).

Cell apoptosis assay

The cells were grown and treated with or without N25 for 48h. The cell apoptosis detected result included two part of the DNA fragmentation and Annexin V-FITC/PI staining assay (GA107)-FITC apoptosis detection kit, Nanjing key gen technology development co., LTD). DNA fragmentation was detected as described in the DNA Ladder assay kit. Annexin V-FITC/PI staining assay was accomplished with the operating manual (Nanjing keygen technology development co. LTD). The cells were analysed on a flow cytometer (Beckman FC500/COULTER EPICS X, Beckman Coulter.inc).

Pharmacokinetics organization distribution and LD_{50} study

To explore the distribution of N25 in the brain and lung tissue of mice. A reverse HPLC method of N25 was developed. Different doses of N25 were injected to mice by intraperitoneal (IP) injection, and the concentration of N25 in brain and lung obtained at different time was determined by HPLC. Mice (6-week-old) were obtained from the Guangzhou University of Chinese Medicine. All experiments were performed under protocols approved previously. Each mouse was injected 600mg/kg, 0.1ml/20g of N25 (DMSO), intraperitoneal (IP) injection. At 5, 15, 30, 60, 90, 120, 180min, mice brain and lung tissue homogenate were measured by HPLC. 60 mice were randomized into six groups (n=10) and received 160, 170, 180, 190, 200, 220, 230mg/kg of body mass N25 by gavage for 7days. The number of death and physical condition were measured every day. Calculated the LD_{50} by the death rate in each group.

Data statistics and analysis

All of the data analysis were conducted according to the type of statistical methods. Most data are displayed as mean±SD. There was very significant difference between both the measure values (p<0.05).

Results

N^1- (2, 5-dimethoxyphenyl)-N^8-hydroxyoctanediamide (N25) is white powder, by ferric chloride solution to generate different oxime hydroxyl acid reaction, purple. MP: 107.0°C-108.2°C. ^{1}HNMR (400MHz, DMSO): δ=10.34 (s, 1H), 8.82 (d, 2H), 7.70 (s, 1H), 7.10-6.35 (m, 2H), 3.52 (m, 3H), 3.37 (d, 2H), 2.44 (d, 3H), 1.95 (d, 2H), 1.57-1.01 (m, 8H). MS (ESI$^+$) m/z: 325.1774 (100%,

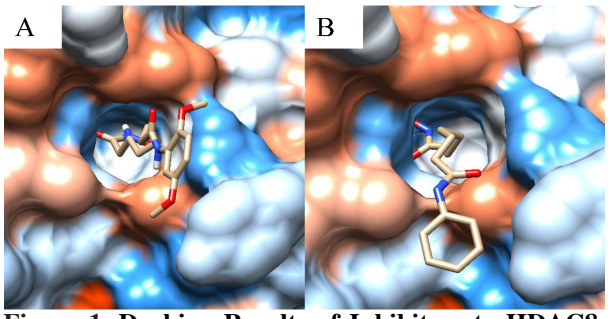

Figure 1. Docking Results of Inhibitors to HDAC8. **A)** Predicted binding of N25 to HDAC8. HDAC8 (PDB code 1T69) is represented as a solid surface and is oriented to illustrate the interaction with N25. The color code corresponds to hydrophilicity, ligands are shown as sticks. **B)** Predicted binding of N25 to HDAC8. AUTODOCKING 4.5.2 was used to predict the mode of binding of SAHA as described in the Experimental Section

Table 1. In vitro Cell Proliferation Inhibition IC_{50}±SD [μM]

Group	U251	U87	T98G	H460	A549	H1299
N25	6.28±0.89	11.33±0.51	15.44±1.01	2.44±0.31	3.46±0.84	2.93±0.64
SAHA	6.32±1.27	6.41±0.08	10.04±2.00	5.16±0.97	7.20±1.29	6.87±1.13

Table 2. The Concentration of N25 in Brain and Lung Obtained at Different Time

Group	Sampling time	Brain homogenate (mg/L)	Lung homogenate (mg/L)
Control sample	180 min	0	0
N25 (600 mg/kg)	5 min	0	1.12±0.03
	15 min	1.55±0.01	1.30±0.02
	30 min	1.57±0.01	1.72±0.43
	60 min	1.80±0.36	2.30±0.63
	90 min	1.58±0.02	1.69±0.41
	120 min	1.58±0.01	1.58±0.56
	180 min	1.60±0.11	1.21±0.20

(M + H^+)). Structure: RNHCO (CH_2)6CONHOH (R=2, 5dimethoxyaniline) with molecular weight 324.17.

N25 is a novel synthetic Suberoylanilide Hydroxamic Acid-type HDACi which mainly modified the Cap Group of SAHA. So N25 has a chemical structure similar to the SAHA. N25 has two methoxy group in its benzene ring, whereas SAHA does not has two methoxy group in its benzene ring. We designed a molecular approach for modeling selected SAHA derivatives based on available structural information regarding human HDAC8 in complex with SAHA (PDB code 1T69). For N25, the hydroxamate linker moiety chelated an extremely similar steric conformation in the binding pocket. Docking analysis was used to locate the N25-binding sites within the HDAC8 catalytic core following the protocol described previously. HDAC8 (PDB code 1T69) was represented as a solid surface and was oriented to illustrate the interaction with N25. The color code corresponds to hydrophilicity (Figure 1A and B). Ligands are shown as sticks. N25 was found to be stabilized by direct interaction with the HDAC8.

To examine the inhibitory effect of N25 on HDACs, we measured leves of HDACs. It was displayed in vitro that N25 showed nearly an same supression capability of HDACs as SAHA. To examine whether the chemical compound was targeting active, we further evaluated the acetylation of lysine residues on histones H3 and H3-K9. The increased acetylation of histone as expected to restrain HDAC. In both U251 and H460 cells, N25 down-regulated HDAC4 and up-regulated acetylation of histone H3. As shown in as (Figure 2A), we exposed U251 and H460 cells to N25 (0, 3, 6, 12μM) and SAHA (6μM) for 48h and performed western blot analysis using antibodies. Acetylation of histone H3-K9+K14+K18+K23+K27 and histone H3-K9 were significantly increased after treatment with N25. In U251 cells observed SAHA and N25 down-regulated the expression of HDAC4 in a concentration-dependent. N25 and SAHA also remarkably increased the acetylation of H3-K9+K14+K18+K23+K27 and H3-K9. Further, the effect of N25 was stronger than SAHA. In H460 cells, compared with SAHA, N25 increased the acetylation of H3-K9+K14+K18+K23+K27 and H3-K9 in a concentration-dependent manner. In U251 cells, the

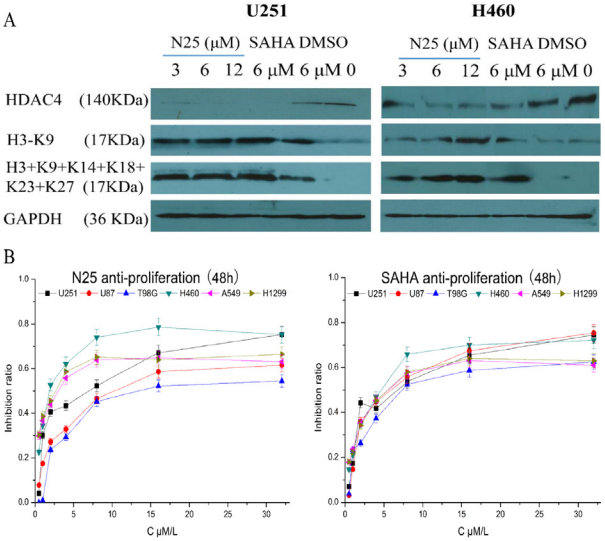

Figure 2. (A) Effects of N25 and SAHA on Acetylation of H3 and Inhibition of HDAC4. Both Human H460 and U251cell lines were treated with SAHA, DMSO at indicated doses and N25 (0, 3, 6, 12μM) for 48h. Western blotting detecting acetylated histone 3 (H3-K9+K14+K18+K23+K27, H3-K9) and HDAC4 levels by N25 to the extents similar to those observed when SAHA were used. The corresponding GAPDH levels are shown as loading controls. **(B) Effect of N25 on the Growth of Cancer Cells *in vitro*.** Human glioma U251, U87, T98G cells and human lung cancer H460, A549, H1299 cells were treated with either N25 at various concentrations (0.5-32μM) or SAHA (control) for 48h. Results are expressed as the percent proliferative response after normalization to solvent (DMSO) treated cells p<0.001, mean±SD of three independent experiments with triplicate dishes

effect of N25 was also stronger than SAHA. In conclusion, N25 treatment and positive control of SAHA showed significantly inhibition of HDAC4 protein expression and promotion of total histone H3 and the acetylation of histone H3-K9 single locus expression levels. These data demonstrate that N25 is a HDACi that results in increased acetylation of histone H3 and H3-K9 at several lysine residues in both H460 and U251 cells.

N25 inhibits cell proliferation and induces cell-cycle arrest

To compare the effects of N25 on cancer cell proliferation with SAHA, the human glioma U251, U87, T98G cells and human lung cancer H460, A549, H1299 cells, were exposed to 0.5, 1.0, 2.0, 4.0, 8.0, 16.0 and 32.0μM of HDACi for 48h. Growth inhibitory efficiency are presented as inhibitory concentration at 50% (IC_{50}) values. Dramatically, N25 suppressed growth of a wide range of cancer cell lines at low concentrations (Figure 2B). Compared with SAHA, N25 has stronger effects on inhibiting U251, H460, A549, H1299 cells proliferation, whereas this efficiency was weaker than SAHA in U87, T98G cells (Table 1). To further investigate the molecular

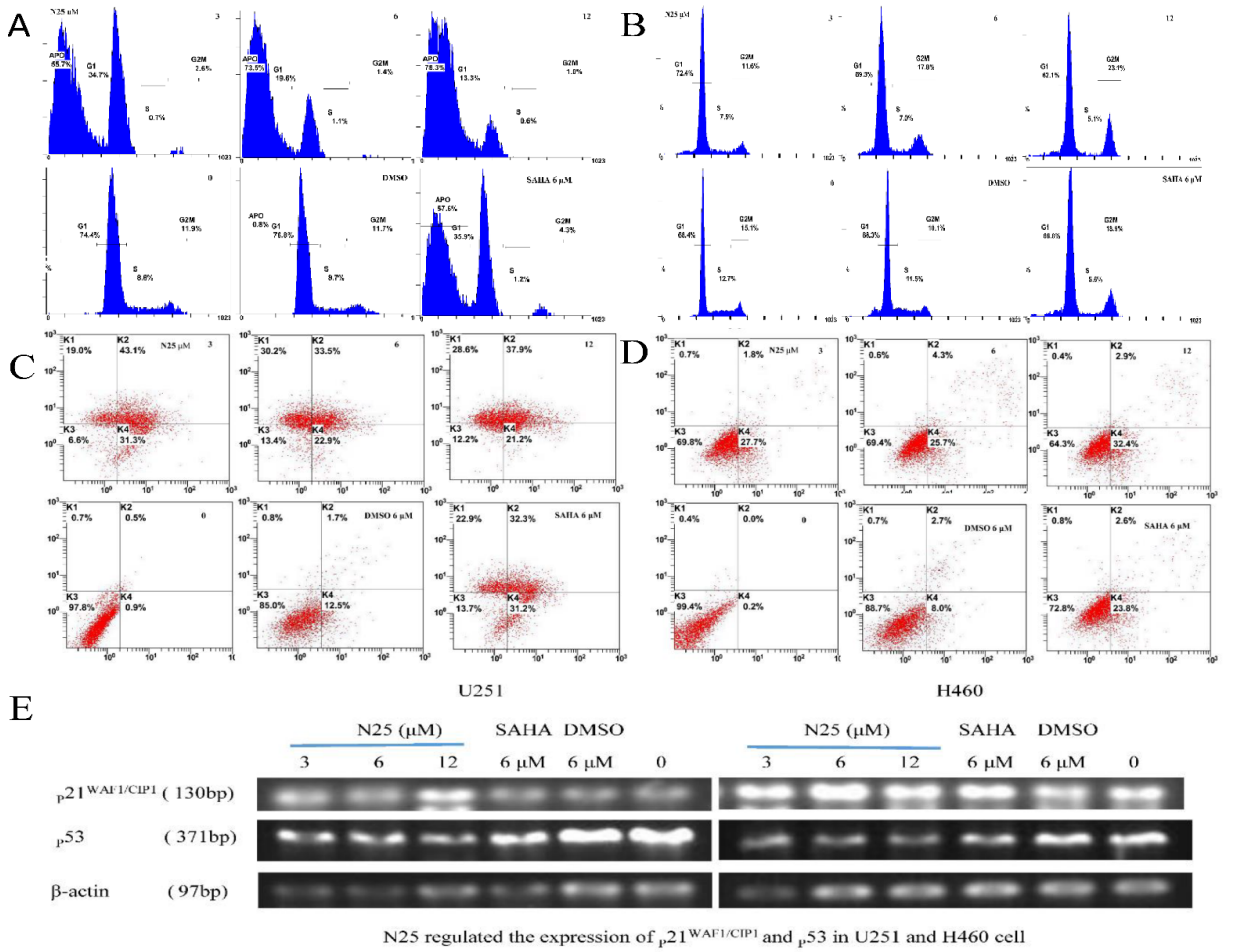

N25 regulated the expression of p21WAF1/CIP1 and p53 in U251 and H460 cell

Figure 3. (A, B) Cell-Cycle Analysis of U251 Cells and H460 Cells by flow Cytometry. A) The effect of N25 induced cell -cycle arrest in U251 cell at G0/G1 stage arrest for 48h. And APO was big, indicated the N25 induction of apoptosis. **B)** In H460 cells suppressed at G2/M stage for 48h. (C, D) Cell death measured by annexin V and PI staining detected by flow cytometry. U251 and H460 cells were treated with N25 for 48h. Cells were then stain with annexin V and PI. The positive cells were positive for annexin V staining while negative for PI staining. **C)** N25 induced apoptosis in U251 cells. **D)** N25 induced apoptosis in H460 cells. Both N25 and SAHA could induce apoptosis in H460 and U251 cells. In U251 cell apoptosis mostly appeared at middle period and in H460 cell apoptosis mostly appeared at early period. **E)** RT-PCR to detect p21WAF1/CIP1 and p53 of U251 and H460 cells treated with N25 and SAHA for the indicated times. Both N25 and SAHA increased the express of p21WAF1/CIP1 in U251 and H460 cells. However, compared with the solvent control and negative control group, p53 gene expression level was lower, these indicated the expression of p21WAF1/CIP1 might not-dependent on way of p53

mechanism of N25, cell-cycle analysis was performed. Respectively treated U251 and H460 cells with N25, induced G0/G1 stage arrest in U251 cells and G2/M arrest in H460 for 48h (Figure 3A). A previous study showed that p21 is one of the target genes that could be regulated by acetylation levels of histone proteins, and induction of p21 protein levels in the cells could cause cell cycle arrest. We therefore determined whether N25 has such an effect by conducting a cell cycle analysis. As shown in Figure 3E, RT-PCR analysis indicated that p21WAF1/CIP1 expression was up-regulated and p53 was down-regulated after N25 treatment, which was consistent with the cell-cycle analysis. As the changes in p21WAF1/CIP1 were much more significant than p53, p21WAF1/CIP1 was up-regulated in H460 and U251 cells. This suggests the p21WAF1/CIP1 expression may be independent of p53 pathway.

N25 induces apoptosis

In general, cell cycle arrest could lead to cell apoptosis or senescence, and other HDAC inhibitors (such as SAHA) have been shown to induce apoptosis in different tumor cells, anti-cancer drugs cause apoptotic cell death at elevated concentrations and thus we investigated whether N25 causes apoptosis in H460 and U251 cells. As shown in Figure 3B, inhibition of cell viability was observed in both H460 and U251 cells in a concentration and time-dependent manner after treated with N25. Moreover, in U251 cells, apoptosis most appeared in medium and late phase, but in H460 cells, apoptosis most appeared in early phase.

Pharmacokinetics organization distribution and LD_{50} study

The linear range of brain was 0.075-2 mg/L (r>0.999). N25 was detected in brain of mice and peak concentration (1.80±0.36mg/L) of N25 appeared at 60min after injection. And the linear range of lung was 0.075-2mg/L (r>0.999). N25 was detected in lung of mice and peak concentration of N25 appeared at 60min after injection. Otherwise, we

discovered that N25 was able to distribute the lung and brain tissue through the blood-brain barrier of mice (Table 2). With SPSS statistical software, the LD_{50} of N25 in mice was estimated to be 240.840mg/kg, intraperitoneal (IP) injection.

Discussion

HDACis have grown into a crucial chemotherapy anticancer agents because of their ability to induce cell cycle arrest and apoptosis, reversible regulated in many malignancies (Ammerpohl et al., 2004; Osada et al., 2005), since FDA approval for the treatment of advanced cutaneous T-cell lymphoma in 2006, including glioma and lung cancer. Although there are many HDACis has conducted the clinical trials, the systemic side effects is a key to the question of these chemotherapy agents. (Hrebackova et al., 2009).

The preliminary examined for their anti-proliferative and histone deacetylation activities in a cell-based assay showed initial efficacy of N25 in glioma and lung caner cells. The anti-proliferative activites of various SAHA derivatives were further investigated in various tumor-derived cell lines. Surprisingly, compared to SAHA, N25 displayed more efficient anti-proliferative activity toward the cell line U251, H460, A549, H1299. As expected, the anti-proliferative activity of the N25 compound correlated well with the cap modified. Our ex-vivo and in-vivo determined that N25 is a HDACi and a promising drug for the treatment of tumor. N25 induced growth arrest, apoptosis and differentiation in H460 and U251 cells in a time and dose dependent manner. As expected, the anti-proliferative activity of the various compounds correlated well with their time-course ability to increase histone H3 acetylation and p21/WAF1 expression. (Xia et al., 2008).

N25, a novel HDACi, is a new modified cap group suberoylanilide hydroxamic acid derivative that has a similar chemical structure to SAHA. But N25 has a specia fork structure of C-O-C at the benzene ring, at the position shows a potentially function of C-O-C (Feng et al., 2013), which might be responsible for the specific binding when N25 was administered to HDAC (Di Micco et al., 2008). The results also suggest that the steric hindrance generated and hydrophobic nature of these groups constitute the most important factors to be taken into consideration during the design of most potent SAHA analogues. Therefore, compared with SAHA, N25 displays lower toxicity, better tolerance and more stability during administration to animals.

According to the above advantage of structure, as for other HDAC inhibitors, N25 was able to anti-proliferative and upgrade acetylation levels of histone proteins in the glioma and lung cancer cell lines. In anti-proliferative test, we selected Cell Counting Kit 8 (CCK-8) insteaded of MTT assay. Because of the amount of the formazan dye, generated by the activities of dehydrogenases in cells, is directly proportional to the number of living cells. The detection sensitivity of CCK-8 is higher than the other tetrazolium salts such as MTT.

N25 also showed some effect on cell cycle arrest, induced G2/M arrest in H460 cells, but suppressed G0/G1 stage arrest for 48h in U251 cells is likely to account for this effect. p21WAF1/CIP1 and p53 are cyclin-dependent kinase inhibitors that important roles in blocking the cell cycle in both G2/M and G0/G1 phase. A possible interpretation is that many anti-tumour drugs have multi-functions and multi-targets. N25 might have some other pathways leading to cell-cycle arrest like enhancing p21WAF1/CIP1 expression level (Figure 3E) and differentiation (Shinji et al., 2006). The other reason was that N25 only inhibited some parts of HDAC activity at low concentration, and it would inhibit more HDAC activity at high concentration. More important, it was found that N25 exposed similar dose-dependent effects on cells. N25 mediated growth arrest and increased expression of differentiation markers (p21WAF1/CIP1), which probably combine to modulate the activity of the downstream pRb/E2F axis, triggering cell cycle arrest. When p21 downgraded (Eymin et al., 2003), Cyclin D, CDK4/CDK6 compounds of prophase promoted the phosphorylation formation of the downstream gene Rb protein, subsequently phosphorylation of Rb released transcription factor E2F thus promoted the transcription of cell cycle factors such as CyclinE/A/B, CyclinE-CDK2 compounds formed in the late, promoted cells by G1/S limit point into the S phase, that was an evolution of the cell cycle. However, the increased p21WAF1/CIP1 inhibited Cyclin kinase, the Rb protein phosphorylation would not work (Ito et al., 2001), so that the absented of transcription factor E2F leaded to cell cycle arrest in a certain stage, the corresponding cell cycle proteins also was affected. Although N25 inhibited HDAC4 expression (Li et al., 2013) and increased acetylation of histone H3, might loose the chromatin structure, leaded the transcription factors into DNA binding sites, promoted a variety of gene transcription (such as p21WAF1/CIP1 gene). These findings showed N25 regulated HDAC at the up-stream of the p21WAF1/CIP1, had a much more complicated regulation mechanism than previous conjecture.

We have demonstrated that N25 is highly effective in inducing apoptosis and suppressing the growth of H460 and U251 cells, although anti-proliferation and apoptosis were independently regulated in tumor cell, anti-proliferation may be associated with apoptosis (Wanczyk et al., 2011), and the effect of anti-proliferation may be combined with intensive chemotherapy to improve the susceptibility of tumor to drug-induced apoptosis (Darvas et al., 2010). Previously, APO was found to be essential for activation of differentiation in H460 and U251 cells. In the present study, we have demonstrated that N25 was not only involved in apoptosis (Miller et al., 2007; Yoshioka et al., 2013), but also in cell differentiation. These mutations may restrain tumor cell growth advantages and induce apoptosis. These events are associated with the accumulation of acetylated H3 and deacetylated HDAC4, confirming that N25 acts as an HDAC inhibitor in these human cancer cell lines.

Though N25 has displayed prominent anti-cancer effects, the more detailed mechanisms are still to be researched. In the present study indicates that N25 is a HDACi with potential antineoplastic agent by way of suppressing cell proliferation, inducing cell cycle

arrest and apoptosis in human tumor cells, these effects are associated with the accumulation of inhibition of histone and non-histone protein acetylation. Further, in the pharmacokinetics organization distribution and LD_{50} study, showed N25 was able to distribute the lung and brain tissue through the blood-brain barrier of mice and peak concentration appeared at 60min in brain of mice after injection (Li et al., 2011). Compared with SAHA, the LD_{50} of N25 in mice: 240.840mg/kg display a particularly hypotoxicity (Kerr et al., 2010). Results indicates N25 can be potentially used in glioma treatment.

In conclusion, our current study demonstrates that N25 is a novel HDAC inhibitor with potential therapeutic values in several malignancies via the inhibition of cell proliferation, inducing differentiation and apoptosis in human tumor cells. Currently, N25 had tested the treatment of various forms of cancer, and the present study indicates that this compound should be considered for the treatment of glioma and lung cancer. In future research, we will focus on the therapeutic role of N25 in vivo for the treatment of H460 and U251 on comparing the potency and efficacy of N25 with other famous HDAC inhibitors. Compared with SAHA, N25 displays an improved antitumor activity in U251 and H460 cells, significantly increased acetylation of histone 3 and inhibited HDAC4. N25 also can distribute the brain tissue through the blood-brain barrier of mice (better tolerance and more stability during administration to animals) with lower toxicity (LD_{50}: 240.840mg/kg). The development of novel HDACis will significantly accelerate the discovery of anti-tumour agents and improve cancer therapy.

Acknowledgements

The authors gratefully acknowledge financial support from the Guangdong Provincial Science and Technology Project (No. 2010B031600137) and Guangdong Pharmaceutical University.

References

Al-Yacoub N, Fecker LF, Mobs M, et al (2012). Apoptosis induction by SAHA in cutaneous T-cell lymphoma cells is related to downregulation of c-FLIP and enhanced TRAIL signaling. *J Invest Dermatol*, **132**, 2263-74.

Ammerpohl O, Thormeyer D, Khan Z, et al (2004). HDACi phenylbutyrate increases bystander killing of HSV-tk transfected glioma cells. *Biochem Biophys Res Commun*, **324**, 8-14.

Darvas K, Rosenberger S, Brenner D, et al (2010). Histone deacetylase inhibitor-induced sensitization to TNFalpha/TRAIL-mediated apoptosis in cervical carcinoma cells is dependent on HPV oncogene expression. *Int J Cancer*, **127**, 1384-92.

Di Fiore A, Maresca A, Supuran CT, De Simone G (2012). Hydroxamate represents a versatile zinc binding group for the development of new carbonic anhydrase inhibitors. *Chem Commun (Camb)*, **48**, 8838-40.

Di Micco S, Chini MG, Terracciano S, et al (2013). Structural basis for the design and synthesis of selective HDAC inhibitors. *Bioorg Med Chem*, **21**, 3795-807.

Di Micco S, Terracciano S, Bruno I, et al (2008). Molecular modeling studies toward the structural optimization of new cyclopeptide-based HDAC inhibitors modeled on the natural product FR235222. *Bioorg Med Chem*, **16**, 8635-42.

Dubois F, Caby S, Oger F, et al (2009). Histone deacetylase inhibitors induce apoptosis, histone hyperacetylation and up-regulation of gene transcription in Schistosoma mansoni. *Mol Biochem Parasitol*, **168**, 7-15.

Duo J, Ma Y, Wang G, Han X, Zhang C (2013). Metformin synergistically enhances antitumor activity of histone deacetylase inhibitor trichostatin a against osteosarcoma cell line. *DNA Cell Biol*, **32**, 156-64.

Ellis L, Pan Y, Smyth GK, et al (2008). Histone deacetylase inhibitor panobinostat induces clinical responses with associated alterations in gene expression profiles in cutaneous T-cell lymphoma. *Clin Cancer Res*, **14**, 4500-10.

Eymin B, Leduc C, Coll JL, Brambilla E, Gazzeri S (2003). p14ARF induces G2 arrest and apoptosis independently of p53 leading to regression of tumours established in nude mice. *Oncogene*, **22**, 1822-35.

Feng T, Wang H, Su H, et al (2013). Novel N-hydroxyfurylacrylamide-based histone deacetylase (HDAC) inhibitors with branched CAP group (Part 2). *Bioorg Med Chem*, **21**, 5339-54.

Finnin MS, Donigian JR, Cohen A, et al (1999). Structures of a histone deacetylase homologue bound to the TSA and SAHA inhibitors. *Nature*, **401**, 188-93.

Hoshino I, Matsubara H (2010). Recent advances in histone deacetylase targeted cancer therapy. *Surg Today*, **40**, 809-15.

Hoshino I, Matsubara H, Akutsu Y, et al (2007). Gene expression profiling induced by histone deacetylase inhibitor, FK228, in human esophageal squamous cancer cells. *Oncol Rep*, **18**, 585-92.

Hrebackova J, Poljakova J, Eckschlager T, et al (2009). Histone deacetylase inhibitors valproate and trichostatin A are toxic to neuroblastoma cells and modulate cytochrome P450 1A1, 1B1 and 3A4 expression in these cells. *Interdiscip Toxicol*, **2**, 205-10.

Ito N, Sawa H, Nagane M, et al (2001). Inhibitory effects of sodium butyrate on proliferation and invasiveness of human glioma cells. *Neurosurgery*, **49**, 430-6, 436-7.

Kerr JS, Galloway S, Lagrutta A, et al (2010). Nonclinical safety assessment of the histone deacetylase inhibitor vorinostat. *Int J Toxicol*, **29**, 3-19.

Li XH, Huang ML, Wang SM, Wang Q (2013). Selective inhibition of bicyclic tetrapeptide histone deacetylase inhibitor on HDAC4 and K562 leukemia cells. *Asian Pac J Cancer Prev*, **14**, 7095-100.

Li Y, Liu B, Fukudome EY, et al (2011). Identification of citrullinated histone H3 as a potential serum protein biomarker in a lethal model of lipopolysaccharide-induced shock. *Surgery*, **150**, 442-51.

Miller CP, Ban K, Dujka ME, et al (2007). NPI-0052, a novel proteasome inhibitor, induces caspase-8 and ROS-dependent apoptosis alone and in combination with HDAC inhibitors in leukemia cells. *Blood*, **110**, 267-77.

Nelson HH, Marsit CJ, Christensen BC, et al (2012). Key epigenetic changes associated with lung cancer development: results from dense methylation array profiling. *Epigenetics*, **7**, 559-66.

Osada H, Tatematsu Y, Sugito N, Horio Y, Takahashi T (2005). Histone modification in the TGFbetaRII gene promoter and its significance for responsiveness to HDAC inhibitor in lung cancer cell lines. *Mol Carcinog*, **44**, 233-41.

Shinji C, Maeda S, Imai K, et al (2006). Design, synthesis, and evaluation of cyclic amide/imide-bearing hydroxamic acid derivatives as class-selective histone deacetylase (HDAC) inhibitors. *Bioorg Med Chem*, **14**, 7625-51.

Sriraksa R, Limpaiboon T (2013). Histone deacetylases and their inhibitors as potential therapeutic drugs for cholangiocarcinoma - cell line findings. *Asian Pac J Cancer Prev*, **14**, 2503-8.

Takai N, Kira N, Ishii T, et al (2011). Novel chemotherapy using histone deacetylase inhibitors in cervical cancer. *Asian Pac J Cancer Prev*, **12**, 575-80.

Wanczyk M, Roszczenko K, Marcinkiewicz K, et al (2011). HDACi--going through the mechanisms. *Front Biosci (Landmark Ed)*, **16**, 340-59.

Xia G, Schneider-Stock R, Diestel A, et al (2008). Helicobacter pylori regulates p21 (WAF1) by histone H4 acetylation. *Biochem Biophys Res Commun*, **369**, 526-31.

Yoshioka T, Yogosawa S, Yamada T, Kitawaki J, Sakai T (2013). Combination of a novel HDAC inhibitor OBP-801/YM753 and a PI3K inhibitor LY294002 synergistically induces apoptosis in human endometrial carcinoma cells due to increase of Bim with accumulation of ROS. *Gynecol Oncol*, **129**, 425-32.